Since January 2020 Elsevier has created a COVID-19 resource centre with free information in English and Mandarin on the novel coronavirus COVID-19. The COVID-19 resource centre is hosted on Elsevier Connect, the company's public news and information website.

Elsevier hereby grants permission to make all its COVID-19-related research that is available on the COVID-19 resource centre - including this research content - immediately available in PubMed Central and other publicly funded repositories, such as the WHO COVID database with rights for unrestricted research re-use and analyses in any form or by any means with acknowledgement of the original source. These permissions are granted for free by Elsevier for as long as the COVID-19 resource centre remains active.

Research in Veterinary Science 97 (2014) 623–630

Contents lists available at ScienceDirect

Research in Veterinary Science

journal homepage: www.elsevier.com/locate/rvsc

Differential response of porcine immature monocyte-derived dendritic cells to virulent and inactivated transmissible gastroenteritis virus

Shanshan Zhao, Qi Gao, Jian Lin, Mengfei Yan, Qinghua Yu, Qian Yang *

Key Lab of Animal Physiology and Biochemistry, Ministry of Agriculture, Nanjing Agricultural University, Wei gang 1, Jiangsu, China

ARTICLE INFO

Article history:
Received 4 May 2014
Accepted 15 September 2014

Keywords:
Porcine monocyte-derived dendritic cells (Mo-DCs)
Virulent transmissible gastroenteritis virus
T cell proliferation
NF-κB

ABSTRACT

Exposure of piglets less than 2 weeks of age to virulent transmissible gastroenteritis virus (TGEV) gives rise to mortality as high as 100%, and adult pigs recovering from its infection often become TGEV carriers. These facts suggest an evasion of the immune system by virulent TGEV. In this study, we showed that a virulent TGEV SHXB strain could infect porcine immature monocyte-derived dendritic cells (Mo-DCs), and down-regulate cell surface markers (SLA-II-DR, CD1a and CD80/86). Moreover, SHXB-infected immature Mo-DCs showed low expression of IL-12 and IFN-γ, and also lost the ability to stimulate T cell proliferation. Finally, SHXB inhibited the activation of nuclear factor kappa B (NF-κB) in these cells. Instead, UV-inactivated SHXB (UV-SHXB) had the opposite effects in immature Mo-DCs. In conclusion, the virulent SHXB could severely impair immature Mo-DCs, which might be involved in the pathogenesis of virulent TGEV *in vivo*.

© 2014 Elsevier Ltd. All rights reserved.

1. Introduction

Transmissible gastroenteritis virus (TGEV), a member of *Coronaviridae*, order *Nidovirales* (Masters, 2006), causes a highly contagious enteric infection in pigs (Pritchard et al., 1999). The exposure of piglets less than 2 weeks of age to virulent TGEV gives rise to mortality as high as 100% within 5 to 7 days, and adult pigs recovering from virulent TGEV infection often become TGEV carriers (McGoldrick et al., 1999; Zhang et al., 2007). These clinical features strongly suggest evasion of the immune system by virulent TGEV.

Dendritic cells (DCs), the most powerful antigen-presenting cells, are critical players in intestinal immune defence. Immature DCs, with the powerful ability to capture antigens and the poor ability of presenting antigens, were widely distributed in the entire intestinal mucosa with prominent localisation in the sub-epithelial areas, forming an extensive network monitoring the invasion of pathogens (Haverson et al., 2000). On encountering antigens, these cells capture invading pathogen, and then migrate to T cell-rich areas of lymphoid organs, gradually maturing during migration. Mature DCs stimulate T cell activation and differentiation for initiating immune responses through the expression of major histocompatibility complex, co-stimulatory molecules and the production of cytokines, such as IFN-γ and IL-12 (Spörri and Reis e Sousa, 2005). Recently, reports have shown that infection of DCs with herpes simplex virus type 1 results in defective maturation, hampering the activation of naïve T cells (Boliar and Chambers, 2010). In addition, the measles virus impedes DC-derived IL-12 production, and fails to stimulate naïve T cell activation (Servet-Delprat et al., 2003). Thus, although DCs are important contributors to antiviral immunity, virus infection can impair the immune function of DCs, potentially leading to persistent infections or anergy of the immune system. TGEV mainly infects and replicates in the porcine enterocytes and may encounter sub-epithelial DCs. However, whether virulent TGEV can also impair the function of porcine DCs resulting in the severe damage of piglets is still not completely understood.

In most cells, nuclear factor kappa B (NF-κB) is involved in a number of cellular processes, including immune regulation, inflammatory response and anti-apoptosis effects (Rahman and McFadden, 2011). Some viruses have evolved strategies to interfere with NF-κB activation in order to evade the immune response and increase their replication and viral progeny production, for example, Epstein–Barr virus, hepatitis C virus, human cytomegalovirus and herpes simplex viruses (Blattman et al., 2014; Choi et al., 2006; Taylor and Bresnahan, 2006; Valentine et al., 2010). In addition, Maria Rescigno and colleagues found that inhibition of NF-κB activation could block the maturation of DCs through down-regulation of major histocompatibility complex and co-stimulatory molecules (Rescigno et al., 1998). However, the role of virulent TGEV in NF-κB activation in infected DCs has not yet been reported.

To date, scarce information is available concerning the interaction between porcine conventional DCs and virulent TGEV and

* Corresponding author. Tel.: +86 02584395817; Fax: +86 25 84398669.
E-mail address: zxbyq@njau.edu.cn (Q. Yang).

http://dx.doi.org/10.1016/j.rvsc.2014.09.008
0034-5288/© 2014 Elsevier Ltd. All rights reserved.

UV-inactivated SHXB (UV-SHXB). In this study, the interaction of the virulent TGEV SHXB strain and UV-SHXB with porcine immature Mo-DCs was investigated. We showed that SHXB could infect the immature Mo-DCs, inhibit the maturation of immature Mo-DCs by down-regulating the expression of major histocompatibility complex and co-stimulatory molecules on them, also limit the production of IL-12, IFN-γ and IL-10, and finally suppress the activation of NF-κB in immature Mo-DCs. However, contrasting results were reported in UV-SHXB treated immature Mo-DCs.

2. Materials and methods

2.1. Virus stock

TGEV (SHXB, wild-virulent strain, verified by the animal attack virus test) was provided by the Jiangsu Academy of Agricultural Sciences (JAAS). The virus was propagated in Swine Testicle (ST) cells and purified using a sucrose gradient, as described previously (Krempl and Herrler, 2001). The viral 50% cell tissue infectious dose ($TCID_{50}$) of the purified SHXB strain was calculated using the Reed and Muench method (Haggett and Gunawardena, 1964). The purified virus was irradiated using UV light for 4 h at an optimal cross-linking value (0.120 J/cm^2). The inactivated SHXB (UV-SHXB) was then determined in ST cells by using an anti-TGEV polyclonal antiserum conjugated to fluorescein isothiocyanate (FITC) (VMRD, USA).

2.2. Generation of Mo-DCs

Porcine Mo-DCs were generated as previously reported (Facci et al., 2010). Briefly, porcine peripheral blood mononuclear cells (PBMC) were separated from the blood of six pigs which were negative for TGEV (2 months old, derived from a combination of the Yorkshire, Landrace, and Large White breeds, raised at an experimental animal breeding centre at JAAS, and the negativity of piglets for TGEV was demonstrated using the RT-PCR (data not shown)) by density centrifugation using Histopaque (1.077 g/L) (Sigma, USA). PBMCs were washed three times in RPMI 1640 medium (Gibco, USA), and resuspended in complete RPMI 1640 medium with 10% FBS (MULTIcell, Canada). PBMC were then placed in six-well plates and incubated overnight at 37 °C in 5% CO_2. The non-adherent cells were removed, leaving the adherent monocytes. The monocytes were cultured in complete RPMI 1640 medium containing 20 ng/mL of pIL-4 (BioSource, USA) and 20 ng/mL of pGM-CSF (Invitrogen, USA) at 37 °C in 5% CO_2. Cells were incubated for 5 days to allow differentiation into immature Mo-DCs; complete RPMI 1640 medium was replaced with cytokine-containing medium on day 3. Immature Mo-DCs were harvested on day 5 and resuspended in RPMI 1640 medium.

2.3. SHXB and UV-SHXB infection of immature Mo-DCs

In our preliminary experiment, we chose four concentrations ($TCID_{50}$ = 0.1, 1, 10 and 100) of TGEV SHXB strain interactions with dendritic cells, the best effect of TGEV infected immature Mo-DCs is the concentration of $TCID_{50}$ = 10. Thus, the immature Mo-DCs were inoculated with TGEV SHXB strain and UV-SHXB at a concentration of 10$TCID_{50}$ cell^{-1}. SHXB was adsorbed for 1 h at 37 °C. In order to eliminate the non-absorbed virus, cells were washed five times at 200 × g for 5 min at 37 °C, and resuspended in fresh RPMI 1640 medium containing pIL-4 and pGM-CSF. In addition, immature Mo-DCs were treated with lipopolysaccharide (LPS, 1 μg/mL, Sigma) for positive control, and the mock immature Mo-DCs were used as the negative control. All Mo-DCs were seeded onto six-well plates (5×10^5 cells per well) and cultured for the required incubation period.

2.4. Virus titration assay

SHXB- and UV-SHXB-infected immature Mo-DCs were seeded onto six-well plates (5×10^5 cells per well) and cultured for 2, 9, 24, 48 h. The virus was collected by freezing and thawing the plates three times, and determined by the tissue culture infectious dose 50 ($TCID_{50}$) in ST cells.

2.5. Quantification of SHXB strain M gene mRNA by real-time quantitative RT-PCR

Total RNA was extracted from approximately 5×10^5 of SHXB infected- and UV-SHXB treated-immature Mo-DCs harvested at 12, 24, 48 h p.i. with a commercial kit (TaKaRa, Japan). Then, RT-PCR was performed using an RT-PCR kit (TaKaRa) according to the manufacturer's instructions. To determine the gene expression profiles, individual samples were diluted 1:10 and 2 μL was amplified in a 20 μL reaction containing 10 μL of SYBR Premix™ Ex Taq (TaKaRa), 0.4 μL of ROX dye II and 0.4 μM of each of the forward and reverse gene-specific primers using an ABI 7500 instrument (Applied Biosystems, USA). The TGEV M gene was the target gene (GenBank accession no. *AF302262.1*), and the primers were: FP: gtgcttcctctcgaaggtgt, RP: cccatccagtcgcactactt. Porcine GAPDH gene was used as the internal parameter (GenBank accession no. *NM_001206359.1*). The primers used for this were: FP: tcatcatctctgccccttct, RP: gtcatgagtccctccacgat. The data were analysed using the ABI PRISM 7500 software tool (Applied Biosystems). Quantification of the target gene was determined by relative standard curves. TGEV M gene and Porcine GAPDH plasmids produced a double-standard curve; the Porcine GAPDH quantity at each sampling time was taken as the standard to determine the target genes quantity.

2.6. Detection of phenotype alteration of SHXB- and UV-SHXB-infected immature Mo-DCs by flow cytometric analysis

Mock, SHXB-infected, UV-SHXB-treated and LPS-treated immature Mo-DCs (1×10^5 cells) were respectively transferred to 1.5 mL centrifuge tubes at 24 h p.i., then washed with 0.01 M PBS twice, and incubated for 30 min at 4 °C with appropriate dilutions of the following primary antibodies: FITC-conjugated mouse anti-swine monoclonal antibody to swine histocompatibility leukocyte Ag II-DR (SLA-II-DR, Clone number: 2E9/13) (LifeSpan BioSciences, USA), FITC-conjugated mouse anti-human monoclonal antibody to the co-stimulatory molecules cluster of differentiation 80/86 (CD80/86, fusion protein Human CTLA-4, Clone number:B7-1/B7-2, Ancell Corporation, USA,), FITC-conjugated mouse anti-porcine monoclonal antibody to cluster of differentiation 1a (CD1a, Clone number: 76-7-4) (Abcam, Hong Kong), and PE-conjugated mouse anti-porcine monoclonal antibody to Swine Workshop Cluster 3a (SWC3a, Clone number: 74-22-15) (Abcam). Then, cells were washed twice with 0.01 M PBS. Finally, the cells were suspended in 200 μL PBS, 1×10^4 cells were analysed by flow cytometry (BD FACSVerse, BD, USA) and the results from flow cytometry were evaluated using the percentage of positive cells. Meanwhile, the isotype-matched mouse antibody (Abcam) was added as an isotype control.

2.7. Apoptosis assay

To quantify the apoptosis of immature Mo-DCs infected with the SHXB and UV-SHXB at 24 h p.i, the dual parameter analysis of Annexin V-FITC (Invitrogen) and Propidium iodide (Sigma) were performed. All samples (1×10^5 cells per sample) were labelled with both Annexin V-FITC (2 mg/mL) and PI (50 mg/mL) for 15 min. After washing three times with 0.01 M PBS, these cells were analysed by flow cytometry (BD FACSVerse, BD).

2.8. Viability of cells assay

Mock, SHXB-infected, UV-SHXB-treated and LPS-treated immature Mo-DCs were seeded onto 96-well plates with 100 μL per-well (1×10^6 cells) and cultured for 24 h. After incubation with 25 μL of MTT (1 mg/mL, Sigma) for 4 h at 37 °C, the reaction was stopped by adding an equal volume of lysis buffer (50% DMSO and 20% SDS, pH 7.4). The absorbance was read at 570 nm. Viability of cells was shown as the stimulatory index (SI) calculated according to the following equation: $SI = (OD_{\text{infected well}} - OD_{\text{bank control}})/(OD_{\text{negative well}} - OD_{\text{bank well}})$.

2.9. ELISA

The supernatants from mock, SHXB-infected, UV-SHXB-treated and LPS-treated immature Mo-DCs (1×10^6 cells) were taken at 24 h p.i., and levels of IL-12, IFN-γ and IL-10 were quantified using commercial the enzyme-linked immunosorbent assay (ELISA) kits (R&D Systems, USA), according to the manufacturer's recommendations.

2.10. Mixed leukocyte reaction (MLR)

T cell proliferation stimulated by immature Mo-DCs treated with SHXB and UV-SHXB was evaluated by flow cytometry using the fluorescent dye carboxyfluorescein succinimidyl ester (CFSE) (Sigma). Allogeneic T lymphocytes were isolated from outbred pigs as described above, and were purified and enriched by filtration through nylon wool columns (Burne et al., 2001). Purified T lymphocytes (1×10^7 cells) were stained with 0.1 μM CFSE in RPMI 1640 medium for 15 min at 37 °C in the dark. Meanwhile, immature Mo-DCs were infected with SHXB (at a concentration of 10 $TCID_{50}$ $cell^{-1}$), UV-SHXB (at a concentration of 10 $TCID_{50}$ $cell^{-1}$), or LPS (1 μg) for 24 h in six-well plates; CFSE-labelled T cells then were co-cultured with mock, SHXB-infected, UV-SHXB-treated and LPS-treated immature Mo-DCs at DC/T ratios of 1:1, 1:10, and 1:100. Co-cultures were incubated at 37 °C at 5% CO_2 for 5 days. Finally, the cells were harvested and the fluorescent intensity of the CFSE was determined by flow cytometric analysis.

2.11. Western blot analysis

All group cells were lysed in a buffer containing 50 mM Tris–HCl (pH 7.4), 1 mM EDTA, 150 mM NaCl, 1% Nonidet P-40, 1 mM phenylmethylsulphonylfluoride, and 10 μg/mL aprotinin. The extraction and isolation of nuclear and cytoplasmic protein was performed (Wang et al., 2009) using the Nuclear and Cytoplasmic Protein Extraction Kit (Beyotime, Jiangsu, China). The protein concentration was determined by the Bradford assay kit (BioRad Laboratories, Hercules, CA). For this, 25 μg of total protein was separated by SDS-polyacrylamide gel and then transferred to a 0.4 μm PVDF membrane. After blocking with 5% non-fat milk at room temperature for 2 h, the membranes were incubated with rabbit-anti-human NF-κB p65 antibody (human NF-κB had a 90% homology with porcine NF-κB, Santa Cruz Biotechnology, USA, 1:400), rabbit-anti-human IκB-α antibody (human IκB-α had a 97% homology with porcine IκB-α, Santa Cruz Biotechnology, 1:400) and mouse anti-human β-actin (human β-actin had a 99% homology with porcine β-actin, Abcam) for overnight at 4 °C; anti-rabbit and anti-mouse secondary antibodies conjugated to horseradish peroxidase were used at 1:5000 (Santa Cruz Biotechnology). Cross-reactivity was visualised using ECL western blotting detection reagents and then analysed through scanning densitometry by a Tanon Image System.

2.12. Statistical analysis

The statistical analysis was performed using the Statistical Product and Services Solutions (SPSS, Chicago, IL, USA) package). One-way analysis of variance (ANOVA) was used for the group comparisons, and P value of less than 0.05 ($P < 0.05$) was considered statistically significant.

3. Results

3.1. Determination of Mo-DC morphology

Immature Mo-DCs generated from porcine monocytes by incubation with RPMI 1640 medium with pGM-CSF and pIL-4 for 5 days became semi-suspended or suspended, with a round appearance and dendritic processes, and often formed clusters at 5 days (Fig. 1A, arrow). Those stimulated by LPS for 24 h had typical DC-like morphology, including a significant size and irregular shape, presenting either as single cells or in clusters on the cell surface at 6 days (Fig. 1B, arrow).

3.2. Infection of immature Mo-DCs by SHXB

First, we aimed to determine whether the TGEV SHXB strain was able to productively infect immature Mo-DCs. Our results showed that the viral titre of SHXB strain in the immature Mo-DCs persistently increased over time, and reached a peak of 10^3 $TCID_{50}$ at 24 h p.i., before gradually decreasing at 48 h p.i. (Fig. 1C). However, no viral titre was detected in the UV-SHXB-treated immature Mo-DCs. This result is consistent with the results showing the expression of SHXB and UV-SHXB M genes in immature Mo-DCs with time (Fig. 1D). The results indicated that the SHXB strain was able to infect immature Mo-DCs at a lower level, while UV-SHXB was not.

3.3. Phenotypic changes of immature Mo-DCs infected with SHXB and UV-SHXB

To investigate the effect of virulent SHXB strain and UV-SHXB infection on the maturation and activation of immature Mo-DCs, the expression of SWC3a, CD1a, CD80/86, and SLA-II-DR molecules on the cells after viral infection for 24 h was examined by flow cytometry. The results showed that the expression of $SWC3a^+CD1a^+$, $SWC3a^+CD80/86^+$, and $SWC3a^+SLA\text{-}II\text{-}DR^+$ in mock immature Mo-DCs was 73.25% ± 2.64, 50.83% ± 1.52, and 50.6% ± 8.99, respectively (Fig. 2A and B). Their surface markers were significantly increased when they were stimulated by LPS for 24 h, and $SWC3a^+CD1a^+$, $SWC3a^+CD80/86^+$, and $SWC3a^+SLA\text{-}II\text{-}DR^+$ were 90.25% ± 4.52, 89.7% ± 3.41, and 79.75% ± 1.6, respectively (Fig. 2A and B). Strikingly, after 24 h of virulent SHXB infection, the surface expression of CD1a, CD80/86 and SLA-II-DR drastically reduced compared with that seen in mock immature Mo-DCs (Fig. 2A and B), while those on immature Mo-DCs treated with UV-SHXB showed more notable up-regulation than mock and SHXB-infected immature Mo-DCs (Fig. 2A and B). These results suggest that virulent SHXB can inhibit the maturation of immature Mo-DCs through the down-regulation of CD1a, CD80/86 and SLA-II-DR, and UV-SHXB can stimulate the maturation of immature Mo-DCs by up-regulating these surface markers. Next, to identify whether the down-regulation of these surface markers in the immature Mo-DCs infected with SHXB was caused by apoptosis, Annexin V and PI were used to detect the early and late apoptosis of Mo-DCs at 24 h p.i. The results showed that SHXB and UV-SHXB infection did not induce early or late apoptosis of the immature Mo-DCs (Fig. 2C), which indicates that immature Mo-DCs infected with SHXB are not related to the apoptosis induced by SHXB infection. In addition, the viabilities of SHXB and UV-SHXB infected cells and LPS stimulated cells were the same

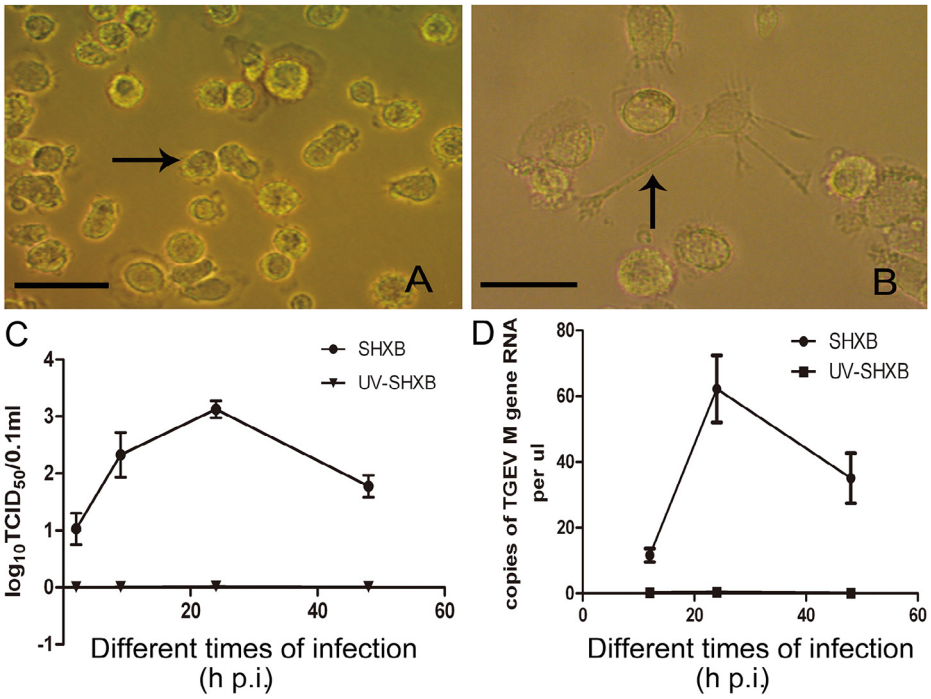

Fig. 1. Morphology of Mo-DCs and infection of TGEV in immature Mo-DCs. Images show the morphology of immature Mo-DCs (A) and mature Mo-DCs (B, immature Mo-DCs treated with LPS for 24 h) by optical microscopy. Scale bars represent 50 nm. (C) The viral titres of TGEV (SHXB) and UV-SHXB in the immature Mo-DCs at 2, 9, 24, and 48 h post infection (p.i.). Data express the mean ± SEM from three independent experiments. (D) The vital M gene RNA copies of SHXB and UV-SHXB in immature Mo-DCs at 12, 24, 48 h p.i. Data express the mean ± SEM from three independent experiments.

as that of mock cells at 24 h p.i. (Fig. 2E), which suggested that SHXB and UV-SHXB could affect the viability of immature Mo-DCs at 24 h p.i.

3.4. Cytokine secretion of immature Mo-DCs infected with SHXB and UV-SHXB

Apart from the fact that co-stimulatory molecules are important players in T-cell activation, cytokines produced by DCs also influence their T-cell stimulatory capacity and their ability to polarise into T cells. The induction of cytokine secretion by immature Mo-DCs after the infection of virulent SHXB and UV-SHXB was analysed. Our results showed that the secretions of IL-12, IFN-γ and IL-10 were highest in LPS-stimulated immature Mo-DCs, followed by UV-SHXB-treated immature Mo-DCs. However, the levels of IL-12, IFN-γ and IL-10 in virulent SHXB infected immature Mo-DCs were equal to or slightly higher than in mock immature Mo-DCs, but significantly lower than in LPS- and UV-SHXB-stimulated cells (Fig. 3A). The results showed that the virulent SHXB strain limited immature Mo-DCs to produce IL-12, IFN-γ and IL-10 to defend against the virus itself, while the UV-SHXB could induce immature Mo-DCs to secrete a considerable amount of IL-12 and IFN-γ for activation of an immune response.

3.5. T cell proliferation stimulated by SHXB- and UV-SHXB-infected immature Mo-DCs

To further investigate any possible functional modulation of virulent SHXB-infected immature Mo-DCs, the viral MHC-restricted antigen-specific T cell response was tested using CFSE staining followed by flow cytometry. The results showed that immature Mo-DCs stimulated by LPS were more stimulatory than others at DC/T cell ratios of 1:1, 1:10 and 1:100 (Fig. 3B). Also, immature Mo-DCs treated with UV-SHXB showed a higher stimulatory capacity than mock immature Mo-DCs at DC/T cell ratios of 1:1, 1:10 and 1:100. However, virulent SHXB-infected immature Mo-DCs had almost no stimulatory capacity with regard to T cell proliferation at DC/T cell ratios of 1:1, 1:10 and 1:100 compared with the mock immature Mo-DCs (Fig. 3B).

3.6. NF-κB translocation in immature Mo-DCs infected with SHXB and UV-SHXB

It has been recognised that NF-κB plays an important role in the regulation of immune and inflammatory responses because of its ability to regulate numerous inducible genes, including those for cytokines, chemokines and adhesion molecules. The mechanism underlying the immunological injury of virulent SHXB-infected immature Mo-DCs was investigated by examining NF-κB translocation using western blot analysis. As expected, there was a significantly higher level of NF-κB p65 in the nucleus of LPS-stimulated and UV-SHXB-infected immature Mo-DCs in comparison to that seen in mock-infected cells at 12 h p.i., while the lowest level of NF-κB p65 was in the nucleus of virulent SHXB infected immature Mo-DCs. Moreover, a contrasting result was found for the level of NF-κB in the cytoplasm and in the nucleus in all groups at 12 h p.i. (Fig. 4, up). This suggests that the virulent SHXB inhibits the NF-κB transcription factor subunits, preventing translocation into the nucleus in immature Mo-DCs, and UV-SHXB enhances this. As IκB of cytoplasm degradation regulates the translocation of NF-κB, we then investigated the degradation of IκB-α in the cytoplasm in this study. Results showed that the cytoplasmic level of IκB-α decreased in the immature Mo-DCs stimulated with LPS and UV-SHXB, while virulent SHXB infection could increase the protein levels of IκB-α at 12 h p.i. (Fig. 4, up). This indicated that virulent SHXB could prevent the degradation of IκB to regulate the translocation of NF-κB. Similarly, the same changes were seen for the expression of NF-κB p65 and IκB-α in immature Mo-DCs of all groups

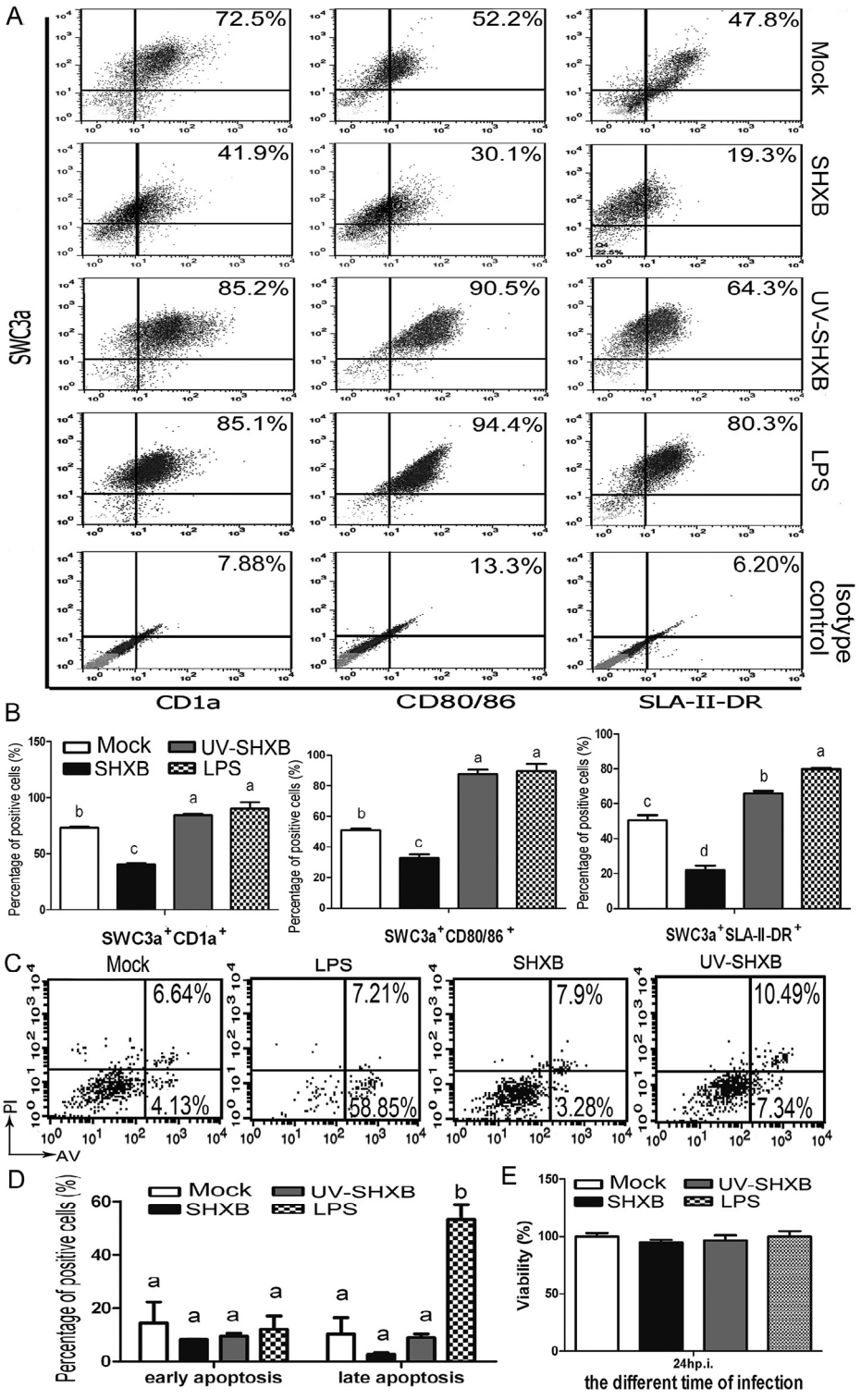

Fig. 2. Expression of CD1a+ SWC3a+, CD80/86+ SWC3a+and SLA-II-DR+ SWC3a+ by immature Mo-DCs infected with virulent SHXB and UV-SHXB at 24 h p.i. and the apoptosis and viability of immature Mo-DCs infected with the SHXB and UV-SHXB at 24 h p.i. (A) Dot plots show the percentage of CD1a+ SWC3a+, CD80/86+ SWC3a+ and SLA-II-DR+ SWC3a+ Mo-DCs in the immature Mo-DCs infected with virulent SHXB and UV-SHXB among the total Mo-DCs at 24 h p.i. (B) Bar graphs show the number of CD1a+ SWC3a+, CD80/86+ SWC3a+ and SLA-II-DR+ SWC3a+ in the immature Mo-DCs infected with SHXB and UV-SHXB. Data express the mean ± SEM from three independent experiments. Bars labelled with different letters are significantly different from each other ($P < 0.05$). (C) Dot plots and (D) bar graphs both show the percentage of apoptotic immature Mo-DCs treated with the SHXB and UV-inactivated SHXB at 24 h p.i. Data express the mean ± SEM from three independent experiments. Bars labelled with different letters are significantly different from each other ($P < 0.05$). (E) Bar graphs show the viability of the immature Mo-DCs infected with SHXB and UV-SHXB. Data express the mean ± SEM from three independent experiments. Bars not labelled with letters are not significantly different from each other ($P > 0.05$).

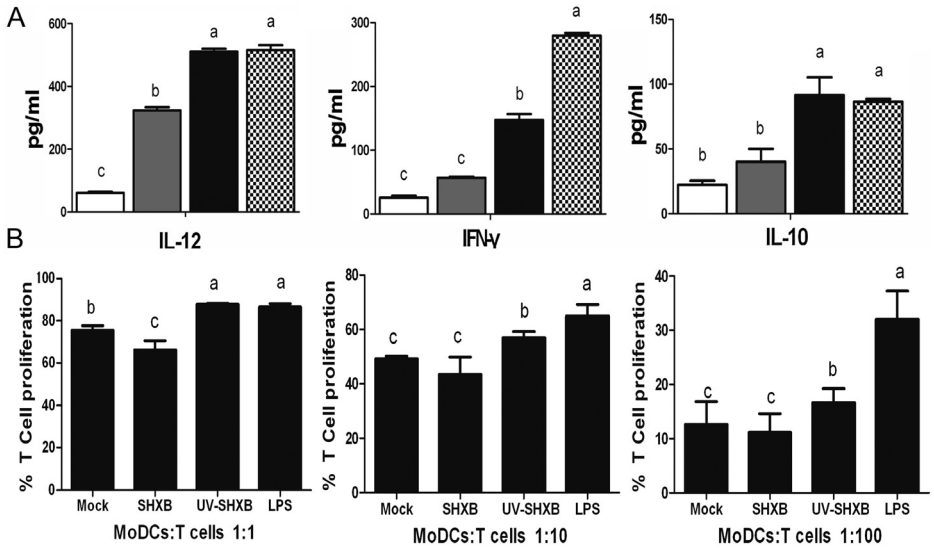

Fig. 3. Inflammatory cytokine production by immature Mo-DCs infected with virulent SHXB and UV-SHXB at 24 h p.i. and T cells activation were stimulated by the virulent SHXB and UV-SHXB infected the immature Mo-DCs. (A) Bar graphs show three inflammatory cytokines (IL-12 (left), IFN-γ (middle), IL-10 (right)) production in the immature Mo-DCs infected with SHXB and UV-SHXB. Data express the mean ± SEM from three independent experiments. Bars labelled with different letters are significantly different from each other ($P < 0.05$). (B) Virulent SHXB- and UV-SHXB infected immature Mo-DCs (24 h p.i.) were co-cultured with T cells at immature Mo-DC:T cell ratios of 1:1 (left), 1:10 (middle), and 1:100 (right). Five days after, co-culture proliferation was evaluated using carboxyfluorescein succinimidyl ester (CFSE). Data express the mean ± SEM from three independent experiments. Bars showing different letters represent values that are significantly different from each other ($P < 0.05$).

between 12 and 24 h of viral infection (Fig. 4, down). Taking all of these results together, it is reasonable to conclude that virulent SHXB failed to activate NF-κB in infected immature Mo-DCs because of the failure of IκB degradation, while UV-SHXB prompted the activation of NF-κB due to increased IκB degradation.

4. Discussion

Neonatal piglet diarrhoea is a major cause of economic losses to modern swine production worldwide. Infection with virulent TGEV forms part of the diarrhoea problem. Recently, progress has been made in understanding the relationship between TGEV and the immune response of piglets, thereby leading to the development of new vaccines. DCs are the first antigen-presenting cells to encounter TGEV at the site of infected intestinal mucosal tissue; thus, it is important to understand the interactions between TGEV and DCs. Some pathogens hijack different parts of the DC immune

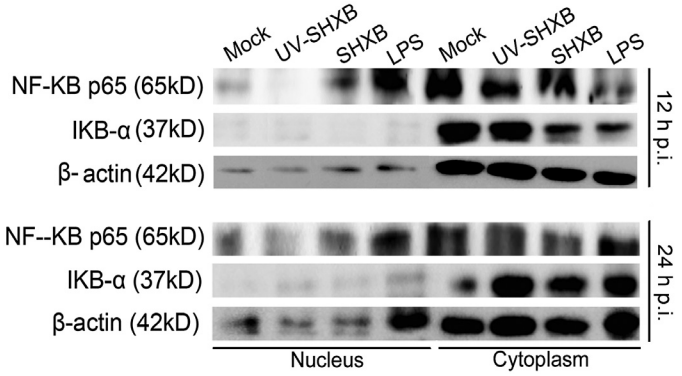

Fig. 4. Effect of SHXB and UV-SHXB infection on NF-κB translocation in immature Mo-DCs. SHXB and UV-SHXB infected immature Mo-DCs for 12 (up) and 24 h (down), and then the protein expressions of NF-κB and IκBα in cytoplasm and nucleus of infected immature Mo-DCs were detected by western blots. β-Actin was used as a loading control.

pathways to escape the host immune response and enhance their survival (Moutaftsi et al., 2002; Smith et al., 2005). The defective function of DCs, including inadequate maturation, reduced antigen presentation capacity, low efficiency of viral-specific T cell response, and imbalance of pro- and anti-inflammatory cytokines, constitutes an important strategy for viruses to evade the host immune system.

Virus infection is the first step in pathogenesis; TGEV can infect porcine alveolar macrophages (PAMs) (Laude et al., 1984). Here, we demonstrated that virulent TGEV could also infect immature Mo-DCs at low levels. It is well known that a common escape mechanism for viruses infecting DCs is to interfere with their maturation process. DC maturation is regarded a pivotal process for the cells to present viral antigens to activate T cells and initiate antiviral immune responses. LPS acts as a DC maturation stimulus in culture, increasing the expression of MHC-II, MHC-I, CD1a, CD80 and CD86, enhancing antigen presentation, and inducing IL-12 production (Langenkamp et al., 2000). As expected, our work found that LPS also stimulated the maturation of immature Mo-DCs. However, virulent SHXB inhibited the maturation of immature Mo-DCs through a reduction of CD1a, CD80/86 and SLA-II-DR, and UV-SHXB stimulated their expression. Our findings are similar to reports stating that influenza A virus (IAV) reduced the amount of CD11c, CD172a, CD1w and CCR5 on DCs (Boliar and Chambers, 2010), while inactivated influenza virus was able to improve the expression of these proteins on DCs (Garulli et al., 2013). Therefore, some structural proteins may play an important role in inducing the maturation of immature Mo-DCs, and some non-structural proteins produced by the TGEV RNA transcription may play an important role in inhibiting the maturation of these immature cells. It is known that viral RNA and some structural proteins, such as spike and membrane, are natural PAMPs that can activate Mo-DCs, while non-structural proteins 3a, 3b and 7 determine the virulence of TGEV. Reports have demonstrated that a deletion of the non-structural protein 3 gene resulted in slightly reduced pathogenicity *in vivo* (Zhang et al., 2007), and removal of non-structural protein 7 promoted an intensified dsRNA-activated host antiviral response (Cruz et al., 2011). The exact reasons for the inhibition of maturation of these immature

Mo-DCs are still not completely understood. Virulent SHXB and UV-SHXB infection could not induce the apoptosis of Mo-DCs at 24 h p.i., which suggests that the down-regulation of surface markers on the Mo-DCs was not caused by apoptosis. This is in agreement with previous studies showing that the severe acute respiratory syndrome virus (SARSV) also did not up-regulate the expression of CD83, CD86, MHC-I and MHC-II on adult immature DCs, and did not induce apoptosis of adult immature DCs (Law et al., 2005).

Besides the expression of surface markers (co-stimulatory molecules and antigen presenting molecules), cytokines produced by DC can contribute to the activation of T cells (Saavedra et al., 2001). Secretion of IL-12 by DCs is critical for the induction of Th1 differentiation, as well as for the proliferation and enhanced cytotoxic activity of natural killer cells (Trinchieri et al., 2003). IFN-γ is an auto-inflammatory cytokine and an important signal for the secretion of IL-12 from DCs, and has immunomodulatory effects on the immune system (Libraty et al., 2001). In addition, IL-10, a predominant Th2-type cytokine, plays a role in immune suppression and has counter-regulatory properties to a number of pro-inflammatory cytokines, including IL-12 (Munoz-Jordan et al., 2003); also, it can induce membrane expression of MHC II molecules on macrophages (Raymond and Wilkie, 2004). We observed that immature Mo-DCs infected with SHXB produced only very low levels of IL-12, IFN-γ and IL-10 compared with LPS- and UV-SHXB-stimulated immature Mo-DCs. This suggests that virulent TGEV-infected immature Mo-DCs would have limited function in inducing Th1 and Th2 response while UV-SHXB stimulated immature Mo-DCs would have a strong ability to promote the Th1 and Th2 response. An inability to secrete IL-12 is also observed in measles virus (MV) and SARSV-infected DCs (Law et al., 2005; Schneider-Schaulies et al., 2003), suggesting that this might be a common immunoevasion strategy. Peak levels of IL-10 secreted by the UV-SHXB-stimulated immature Mo-DCs coincided with peak levels of IL-12 and IFN-γ. It is possible that the higher IL-12 and IFN-γ levels induced could promote IL-10 production in these cells, thereby suppressing the over-stimulation of the immune response by these pro-inflammatory cytokines (Demangel et al., 2002; Mocellin et al., 2003).

The establishment of a robust T cell response is a key factor in determining the consequence of a virus infection. Both the expression of the surface markers as well as the pro-inflammatory cytokines were inhibited by SHXB-infected immature Mo-DCs and induced by UV-SHXB stimulated immature Mo-DCs; thus, the virulent SHXB-infected immature Mo-DCs had a reduced capacity to activate T cells while the UV-SHXB stimulated immature Mo-DCs were more efficient at activating and expanding T cells at a DC/T cell ratio of 1:1 and 1:10 in our work. Interestingly, SHXB-infected immature Mo-DCs and UV-SHXB-stimulated immature Mo-DCs showed no inhibitory or stimulatory capacity at a DC/T cell ratio of 1:100. The major reason for this might be that the lower its presence in Mo-DCs, the weaker its ability to affect T cell proliferation. Thus there is no significant difference among the SHXB-infected, UV-SHXB-stimulated and mock immature Mo-DCs at a DC /T ratio of 1:100.

It is well recognised that the host can utilise NF-κB to trigger defence mechanisms against the virus; however, many viral pathogens also benefit from hijacking NF-κB-driven cellular functions. Mature DCs express high levels of the NF-κB family of transcription factors (Granelli-Piperno et al., 1995); before stimulation, NF-κB is retained in the cytoplasm in an inactive form due to its binding to the inhibitor (IκB) proteins. In response to a number of different stimuli, IκB is degraded and allows NF-kB to translocate to the nucleus and activate the transcription of target genes (Ghosh and Hayden, 2008). The present study demonstrated for the first time that virulent TGEV was not able to activate NF-κB in infected immature Mo-DCs due to the higher level of IκB-α in the cytoplasm, and the lower expression of NF-κB p65 in the nucleus of SHXB-infected immature Mo-DCs. However, UV-SHXB was able to stimulate the activation of NF-κB in immature Mo-DCs by decreasing the level of IκB-α in the cytoplasm and increasing the amount of NF-κB p65 in the nucleus of immature Mo-DCs. We speculate that virulent SHXB might exploit the NF-κB of immature Mo-DCs to optimise their replication or control the proliferation, survival and immune response of immature Mo-DCs. Also, UV-SHXB, not infectious viral particles, stimulated the activation of NF-κB, which could participate in the induction of the immature Mo-DCs maturation and immune response. Similarly, Fang et al. reported that the SARS-CoV M protein physically interacted with Iκκ-β, suppressing IκB-α protein degradation and NF-κB activation (Fang et al., 2007). However, the detailed molecular mechanisms and viral components of virulent TGEV underlying the suppression of NF-κB activation remain to be elucidated.

In conclusion, virulent TGEV SHXB strains could replicate in immature Mo-DCs, and suppress the maturation of immature Mo-DCs by down-regulating the expression of SLA-II-DR, CD80/86 and CD1a, decreasing the secretion IL-12, INF-γ and IL-10 of immature Mo-DCs, and inhibiting their ability to activate and expand T cells. Moreover, SHXB strain infection could inhibit the activation of NF-κB in immature Mo-DCs. However, UV-inactivated SHXB (UV-SHXB) used as a control was able to enhance the expression of surface markers on the immature Mo-DCs and increase the secretion of cytokines, and UV-SHXB-treated immature Mo-DCs could stimulate T cell proliferation. Moreover, UV-SHXB was capable of activating NF-κB in the immature Mo-DCs. The results indicate a possible mechanism for virulent TGEV evasion of innate host defences, providing a basis for understanding the molecular pathways in TGEV pathogenesis. Moreover, UV-TGEV might be a potentially useful vaccine for the activation of immature Mo-DCs.

Acknowledgements

This work was supported by Grant Number 31172302 from the National Science Grant of China, and a project funded by the Priority Academic Program Development of Jiangsu Higher Education Institutions.

References

Blattman, N.N., Lagunoff, M., Corey, L., 2014. Nuclear factor kappa B is required for the production of infectious human herpesvirus 8 virions. Virology 5, 129.

Boliar, S., Chambers, T.M., 2010. A new strategy of immune evasion by influenza A virus: inhibition of monocyte differentiation into dendritic cells. Veterinary Immunology and Immunopathology 136, 201–210.

Burne, M.J., Daniels, F., El Ghandour, A., Mauiyyedi, S., Colvin, R.B., O'Donnell, M.P., et al., 2001. Identification of the CD4(+) T cell as a major pathogenic factor in ischemic acute renal failure. The Journal of Clinical Investigation 108, 1283–1290.

Choi, S.-H., Park, K.-J., Ahn, B.-Y., Jung, G., Lai, M.M., Hwang, S.B., 2006. Hepatitis C virus nonstructural 5B protein regulates tumor necrosis factor alpha signaling through effects on cellular IκB kinase. Molecular and Cellular Biology 26, 3048–3059.

Cruz, J.L., Sola, I., Becares, M., Alberca, B., Plana, J., Enjuanes, L., et al., 2011. Coronavirus gene 7 counteracts host defenses and modulates virus virulence. PLoS Pathogens 7, e1002090.

Demangel, C., Bertolino, P., Britton, W.J., 2002. Autocrine IL-10 impairs dendritic cell (DC)-derived immune responses to mycobacterial infection by suppressing DC trafficking to draining lymph nodes and local IL-12 production. European Journal of Immunology 32, 994–1002.

Facci, M.R., Auray, G., Buchanan, R., Van Kessel, J., Thompson, D.R., Mackenzie-Dyck, S., et al., 2010. A comparison between isolated blood dendritic cells and monocyte-derived dendritic cells in pigs. Immunology 129, 396–405.

Fang, X., Gao, J., Zheng, H., Li, B., Kong, L., Zhang, Y., et al., 2007. The membrane protein of SARS-CoV suppresses NF-κB activation. Journal of Medical Virology 79, 1431–1439.

Garulli, B., Di Mario, G., Sciaraffia, E., Accapezzato, D., Barnaba, V., Castrucci, M.R., 2013. Enhancement of T cell-mediated immune responses to whole inactivated influenza virus by chloroquine treatment in vivo. Vaccine 31, 1717–1724.

Ghosh, S., Hayden, M.S., 2008. New regulators of NF-κB in inflammation. Nature Reviews. Immunology 8, 837–848.

Granelli-Piperno, A., Pope, M., Inaba, K., Steinman, R.M., 1995. Coexpression of NF-kappa B/Rel and Sp1 transcription factors in human immunodeficiency virus 1-induced, dendritic cell-T-cell syncytia. Proceedings of the National Academy of Sciences of the United States of America 92, 10944–10948.

Haggett, P., Gunawardena, K., 1964. Determination of population thresholds for settlement functions by the Reed-Muench method. The Professional Geographer: The Journal of the Association of American Geographers 16, 6–9.
Haverson, K., Singha, S., Stokes, C.R., Bailey, M., 2000. Professional and non-professional antigen-presenting cells in the porcine small intestine. Immunology 101, 492–500.
Krempl, C., Herrler, G., 2001. Sialic acid binding activity of transmissible gastroenteritis coronavirus affects sedimentation behavior of virions and solubilized glycoproteins. Journal of Virology 75, 844–849.
Langenkamp, A., Messi, M., Lanzavecchia, A., Sallusto, F., 2000. Kinetics of dendritic cell activation: impact on priming of TH1, TH2 and nonpolarized T cells. Nature Immunology 1, 311–316.
Laude, H., Charley, B., Gelfi, J., 1984. Replication of transmissible gastroenteritis coronavirus (TGEV) in swine alveolar macrophages. The Journal of General Virology 65 (Pt 2), 327–332.
Law, H.K., Cheung, C.Y., Ng, H.Y., Sia, S.F., Chan, Y.O., Luk, W., et al., 2005. Chemokine up-regulation in SARS-coronavirus-infected, monocyte-derived human dendritic cells. Blood 106, 2366–2374.
Libraty, D.H., Pichyangkul, S., Ajariyakhajorn, C., Endy, T.P., Ennis, F.A., 2001. Human dendritic cells are activated by dengue virus infection: enhancement by gamma interferon and implications for disease pathogenesis. Journal of Virology 75, 3501–3508.
Masters, P.S., 2006. The molecular biology of coronaviruses. Advances in Virus Research 66, 193–292.
McGoldrick, A., Lowings, J.P., Paton, D.J., 1999. Characterisation of a recent virulent transmissible gastroenteritis virus from Britain with a deleted ORF 3a. Archives of Virology 144, 763–770.
Mocellin, S., Panelli, M.C., Wang, E., Nagorsen, D., Marincola, F.M., 2003. The dual role of IL-10. Trends in Immunology 24, 36–43.
Moutaftsi, M., Mehl, A.M., Borysiewicz, L.K., Tabi, Z., 2002. Human cytomegalovirus inhibits maturation and impairs function of monocyte-derived dendritic cells. Blood 99, 2913–2921.
Munoz-Jordan, J.L., Sanchez-Burgos, G.G., Laurent-Rolle, M., Garcia-Sastre, A., 2003. Inhibition of interferon signaling by dengue virus. Proceedings of the National Academy of Sciences of the United States of America 100, 14333–14338.
Pritchard, G.C., Paton, D.J., Wibberley, G., Ibata, G., 1999. Transmissible gastroenteritis and porcine epidemic diarrhoea in Britain. The Veterinary Record 144, 616–618.
Rahman, M.M., McFadden, G., 2011. Modulation of NF-κB signalling by microbial pathogens. Nature Reviews. Microbiology 9, 291–306.
Raymond, C.R., Wilkie, B.N., 2004. Th-1/Th-2 type cytokine profiles of pig T-cells cultured with antigen-treated monocyte-derived dendritic cells. Vaccine 22, 1016–1023.
Rescigno, M., Martino, M., Sutherland, C.L., Gold, M.R., Ricciardi-Castagnoli, P., 1998. Dendritic cell survival and maturation are regulated by different signaling pathways. The Journal of Experimental Medicine 188, 2175–2180.
Saavedra, R., Segura, E., Leyva, R., Esparza, L.A., Lopez-Marin, L.M., 2001. Mycobacterial di-O-acyl-trehalose inhibits mitogen- and antigen-induced proliferation of murine T cells in vitro. Clinical and Diagnostic Laboratory Immunology 8, 1081–1088.
Schneider-Schaulies, S., Klagge, I.M., ter Meulen, V., 2003. Dendritic cells and measles virus infection. Current Topics in Microbiology and Immunology 276, 77–101.
Servet-Delprat, C., Vidalain, P.-O., Valentin, H., Rabourdin-Combe, C., 2003. Measles Virus and Dendritic Cell Functions: How Specific Response Cohabits with Immunosuppression, Dendritic Cells and Virus Infection. Springer, New York, pp. 103–123.
Smith, A.P., Paolucci, C., Di Lullo, G., Burastero, S.E., Santoro, F., Lusso, P., 2005. Viral replication-independent blockade of dendritic cell maturation and interleukin-12 production by human herpesvirus 6. Journal of Virology 79, 2807–2813.
Spörri, R., Reis e Sousa, C., 2005. Inflammatory mediators are insufficient for full dendritic cell activation and promote expansion of CD4+ T cell populations lacking helper function. Nature Immunology 6, 163–170.
Taylor, R.T., Bresnahan, W.A., 2006. Human cytomegalovirus IE86 attenuates virus-and tumor necrosis factor alpha-induced NFκB-dependent gene expression. Journal of Virology 80, 10763–10771.
Trinchieri, G., Pflanz, S., Kastelein, R.A., 2003. The IL-12 family of heterodimeric cytokines: new players in the regulation of T cell responses. Immunity 19, 641–644.
Valentine, R., Dawson, C.W., Hu, C., Shah, K.M., Owen, T.J., Date, K.L., et al., 2010. Epstein-Barr virus-encoded EBNA1 inhibits the canonical NF-κB pathway in carcinoma cells by inhibiting IKK phosphorylation. Molecular Cancer 9, 1.
Wang, J., Du, X.X., Jiang, H., Xie, J.X., 2009. Curcumin attenuates 6-hydroxydopamine-induced cytotoxicity by anti-oxidation and nuclear factor-kappa B modulation in MES23.5 cells. Biochemical Pharmacology 78, 178–183.
Zhang, X., Hasoksuz, M., Spiro, D., Halpin, R., Wang, S., Stollar, S., et al., 2007. Complete genomic sequences, a key residue in the spike protein and deletions in nonstructural protein 3b of US strains of the virulent and attenuated coronaviruses, transmissible gastroenteritis virus and porcine respiratory coronavirus. Virology 358, 424–435.